nature physics

SUPPLEMENTARY INFORMATION

DOI: 10.1038/NPHYS3742

Josephson φ_0-junction in nanowire quantum dots

D. B. Szombati, S. Nadj-Perge, D. Car, S. R. Plissard, E. P. A. M. Bakkers, L. P. Kouwenhoven

DOI: 10.1038/NPHYS3742

1. Breaking of the chiral symmetry in quantum dots

In one-dimensional systems in which the electron momentum is well defined, the interplay between the spin-orbit interaction (SOI) and the Zeeman splitting can create a difference between the dispersion of electrons moving forward and backward. This in turn can lead to the breaking of the chiral symmetry and, in the case of superconducting transport, to Josephson φ_0-junctions [1–3]. In quantum dots (QDs) there is no well-defined momentum since the QD states are localized. Nevertheless, the combination of the SOI and the external magnetic field still creates similar conditions for breaking of the chiral symmetry as shown in Refs. [4–6] and discussed below.

Let us consider a process describing a Cooper pair tunnelling from the left to the right lead (rightward tunnelling) at zero phase difference. Without SOI electrons forming the Cooper pair tunnel through the QD via a single orbital level, for example the first electron tunnels via level 1 and the second via level 2. The corresponding tunnelling coefficient (matrix element) for this process is given by $(t_{L1}t_{R1})(t_{L2}t_{R2})$. Here the t_{L1} and t_{L2} (t_{R1} and t_{R2}) are the hybridization amplitudes between QD levels 1 and 2 with the left (right) lead. The terms in brackets correspond to tunnelling coefficients for individual electrons. Assuming that the hybridization amplitudes are real, the matrix element describing tunnelling from the right to the left (leftward tunnelling) is exactly the same. Since the leftward tunnelling contributes to the current flow in the opposite direction, the net resulting current vanishes. Therefore, the tunnelling via single orbitals can not add to $I(\varphi = 0)$. The lowest order process which contributes to $I(\varphi = 0)$ is the one in which one electron tunnels through the dot directly via a single orbital, while the other electron changes the orbital during the tunnelling process. Finite SOI enables such orbital change.

In the simplest case when two quantum dot levels contribute to Cooper pair transport and the magnetic field is orientated along the effective spin-orbit axis the Hamiltonian of the dot can be written as

$$H_{QD} = (\mu\tau_0 + E_{orb}\tau_z)\sigma_0 + B\tau_0\sigma_z + \alpha\tau_y\sigma_z \quad (1)$$

Here μ is the chemical potential, E_{orb} is the orbital energy, α parametrizes the strength of the SOI and B the Zeeman splitting, $\tau_{X,Y,Z}$ ($\sigma_{X,Y,Z}$) are Pauli matrices acting in orbital (spin) space (τ_0 (σ_0) are identity matrices). Usually the terms describing the Zeeman splitting and the SOI are smaller in comparison to the first term in the Hamiltonian. In the presence of SOI the eigenstates of the QD are mixtures of the two orbital states. This mixture between QD eigenstates and the left (right) lead can be expressed in terms of the single level tunnelling coefficients as $t_{L(R)1'}=t_{L(R)1}\cos\varepsilon + i\sin\varepsilon\, t_{L(R)2}$ and $t_{L(R)2'}= t_{L(R)2}\cos\varepsilon - i\sin\varepsilon\, t_{L(R)1}$ for spin-up electrons (with $\sin\varepsilon = \alpha/E_{orb}$). For the spin down electrons + and - signs should be inverted.

Importantly, due to orbital mixing, the coefficients describing tunnelling events become complex numbers implying that electrons crossing the junction gain a finite phase. This phase is opposite for the electrons tunnelling in the other direction. Therefore the rightward and leftward tunnelling coefficients are not exactly the same (the imaginary part is different) and the two tunnelling processes do not cancel each other. If Cooper pairs also acquire a finite phase during the tunnelling process, $I(\varphi = 0)$ becomes finite. However, if the magnetic field is zero, since spin-up and spin-down electrons obtain the opposite phases in the tunnelling process, Cooper pairs do not gain phase even when SOI is present. For finite magnetic fields the tunnelling probabilities for the tunnelling of spin-

up and spin-down electrons via different orbitals are no longer exactly the same. Only in this case can Cooper pairs obtain a finite phase.

Finally we stress that the complex tunnel coupling between superconductors (occurring due to the combination of SOI and finite magnetic field) always leads to finite $I(\varphi=0)$. Interestingly, this follows even from Feynman's simplified description of the Josephson effect [7]. If we assume that the wave-functions describing the two superconductors are $\psi_L = |\psi_L|e^{i\varphi_L}$ and $\psi_R = |\psi_R|e^{i\varphi_R}$, the time dependent Hamiltonian describing the superconductors on the two side of the junction can be written as

$$i\hbar\frac{\partial}{\partial t}\psi_L = \mu_L\psi_L + T\psi_R$$

$$i\hbar\frac{\partial}{\partial t}\psi_R = T^*\psi_L + \mu_R\psi_R.$$

Here μ_L and μ_R are the chemical potentials in the two superconductors and T is the tunnel coupling. Solving this set of equations for current directly gives

$I \sim |\psi_L||\psi_R|\,(\mathrm{Re}(T)\sin(\varphi_L - \varphi_R) + \mathrm{Im}(T)\cos(\varphi_L - \varphi_R))$.

When T is real current is proportional to $\sin(\varphi)$, with $\varphi = \varphi_L - \varphi_R$. However if the imaginary part is non -zero, the term ~ $\cos(\varphi)$ also contributes to the current and gives rise to the finite $I(\varphi=0)$.

DOI: 10.1038/NPHYS3742

2. Characterization of the quantum dot junction and the nanowire based SQUID

In order to characterize the QD Josephson junction, we performed voltage and current bias measurements while the reference junction was pinched off. Depending on the exact gate configuration, the measured QD resistance varies between 40-600 kΩ and the switching currents are in the range 40-300 pA. In all measurements the sub-gap resistance is finite since the Josephson energy of the QD junction $E_J = \Phi_0 I_C / 2\pi \approx 0.5\text{-}3$ μeV is comparable to $k_B T \approx 5$ μeV. The induced gap in the QD junction is of the order of 20-50 μeV (see Fig. S2 (**b**), (**d**)).

When the reference junction is open we observe standard SQUID oscillations. In this regime it is even easier to resolve small supercurrents of the QD junction by simply estimating the amplitude of the flux dependent voltage oscillations. Note that the data presented in the main text is taken with the SQUID tuned to the overdamped regime. However, at low magnetic fields, the SQUID is usually underdamped (Fig. S3). Due to hysteresis effects, in this case, phase offsets are difficult to track in the voltage vs flux measurements when the current bias is fixed. For this reason, before each measurement we made sure that SQUID is in the overdamped regime by tuning the switching current of the reference junction via G_{ref}.

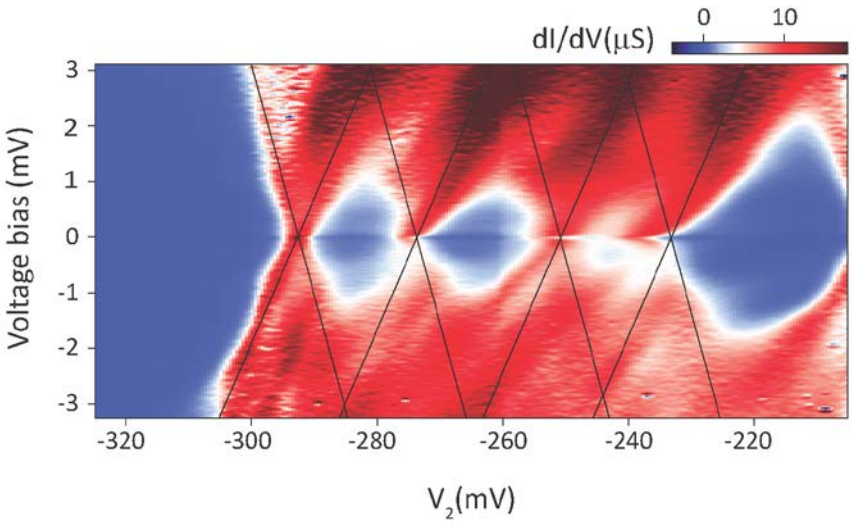

Fig. S1: Coulomb blockade diamonds |Gate configuration is the same as in Fig. 1 and Fig. 2 (V_1 = 350 mV; V_3 = 110 mV).

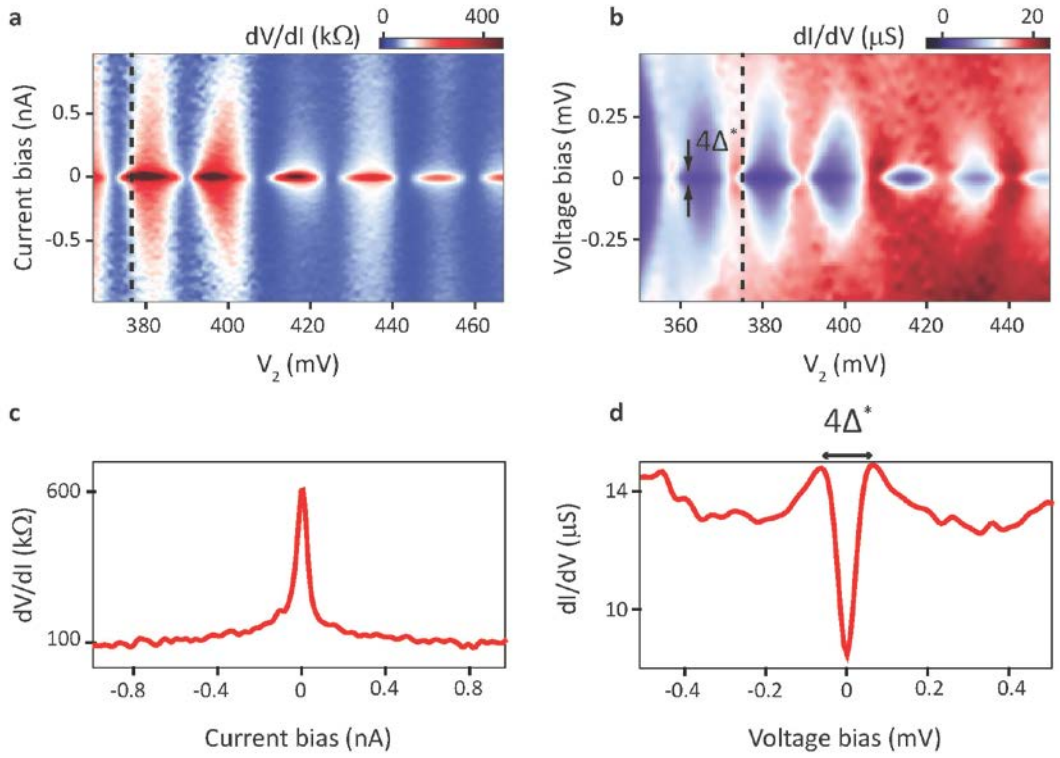

Fig. S2: Superconducting gap in Coulomb blockade | Current biased (**a**) and the corresponding voltage biased (**b**) regime (V_1 = 350 mV; V_3 = 110 mV) vs V_2. In this regime QD has ~30 electrons more compared to Fig. S1**. c**,**d**, Linecuts for current (voltage) bias for the fixed gate voltage showing resistance (conductance) of the QD junction. The sudden increase in resistance corresponds to the suppression of the density of the states inside of the superconducting gap Δ^* ≈ 25 μeV in this regime. Note that the coupling between the QD and the leads is larger compared to Δ^*.

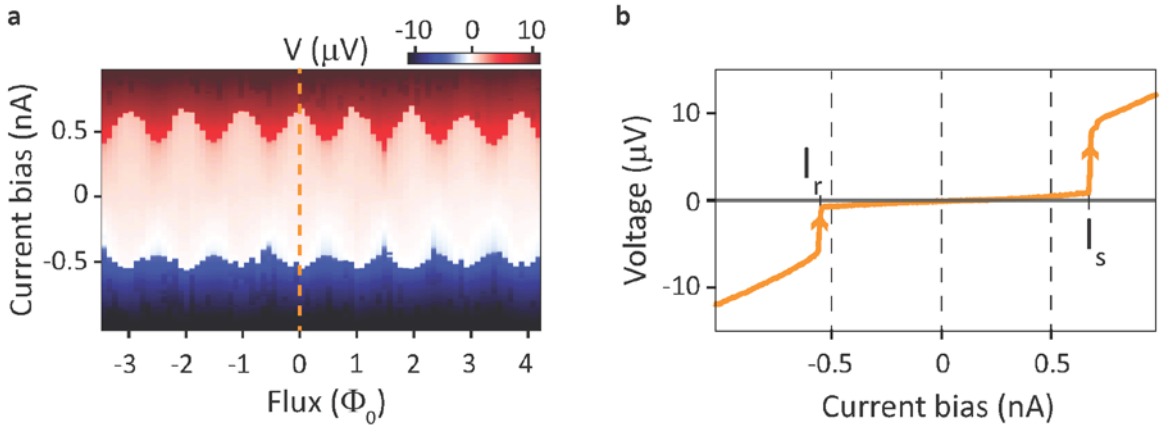

Fig. S3: SQUID in the underdamped regime at zero in-plane field| **a**, Voltage as a function of flux and the current bias showing hysteresis effects in the switching and retrapping current. **b**, Line cut along the dashed line in (**a**) showing a difference of around 200 pA between switching and retrapping currents. Gate setting are: V_1 = 100 mV; V_2 = 25 mV; V_3 = 335 mV; V_{ref} = 420 mV.

DOI: 10.1038/NPHYS3742

3. Anomalous current and direction dependent critical current in φ_0-junctions

The subject of φ_0-junctions has been theoretically extensively studied in the past. They have been predicted to arise in many different systems besides quantum dots [1,5,16], such as conventional superconductors with spin-orbit coupling [17–19], with triplet correlations [20–22], superconductors in contact with topological materials [23,24] and also hybrid systems with nonconventional superconductors [25–27].

The current-phase relation (CPR) for conventional Josephson junctions states that the switching current varies with the sine of the phase difference across the junction: $I_S(\varphi) = I_0 \sin\varphi$, where the junction's critical current $I_C = I_0$. This CPR can be generalized by adding a cosine term:

$$I_S(\varphi) = I_0 \sin\varphi + I_{anomalous} \cos\varphi \equiv I_C \sin(\varphi + \varphi_0),$$

where the critical current is now expressed as $I_C = \sqrt{{I_0}^2 + {I_{anomalous}}^2}$. For conventional 0-junctions ($\varphi_0 = 0$) and π-junctions ($\varphi_0 = \pi$, $I_S(\varphi) = -|I_0| \sin\varphi \equiv I_0 \sin(\varphi + \pi)$), the anomalous term vanishes and there is no current flowing when the phase difference $\varphi = 0$. This can be seen in Fig. S4 (**a**) where we plot the switching current as a function of the phase difference φ for a 0-junction and a π-junction.

It follows that a φ_0 term different from 0 or π directly implies the existence of a finite anomalous current. In Fig.S4 (**b**) we show the anomalous current for a junction with $\varphi_0 = 0.15\pi$. This is a shifted sine curve, hence $I_{C+} \equiv \max_\varphi I_S = I_{C-} \equiv \left|\min_\varphi I_S\right|$, meaning that the critical current is independent of the bias direction. In order to be able to measure a different critical current when the bias is reversed, i.e. to satisfy the condition $I_{C+} \neq I_{C-}$, the CPR needs to contain higher order terms, e.g. as in the experiment by *Sickinger et al.* [15] In Fig. S4 (**c**) we plot the switching current for a junction with $I_S(\varphi) = \sin(\varphi + 0.35\pi) - 0.5 \sin 2\varphi$ and indeed obtain two different critical currents as shown on the plot.

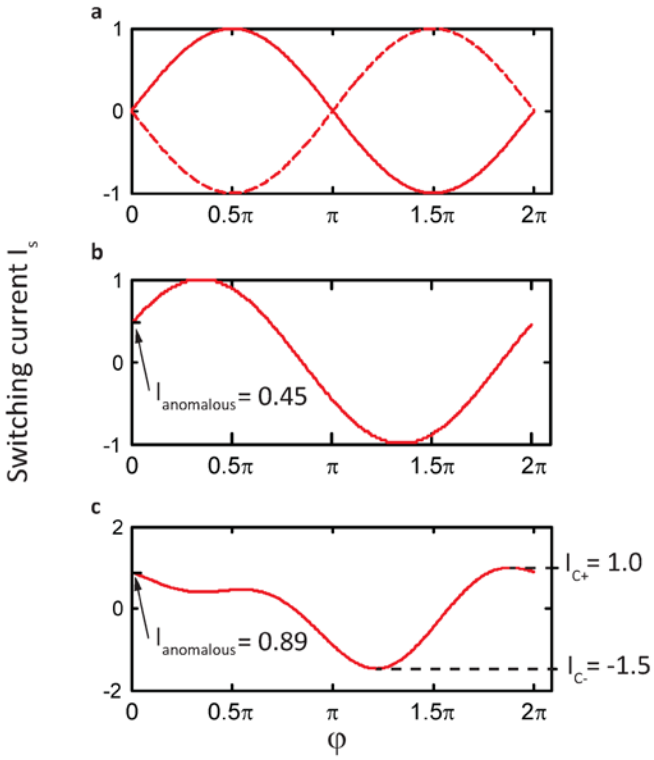

Fig. S4: Switching current for junctions with various CPR normalized to I_0 | a, $I_S(\varphi) = \sin\varphi$ (continuous line) and $I_S(\varphi) = \sin(\varphi + \pi)$ (dashed line). **b**, $I_S(\varphi) = \sin(\varphi + 0.15\pi)$, $I_{anomalous} = I_S(0)$ is shown. **c**, $I_S(\varphi) = \sin(\varphi + 0.35\pi) - 0.5\sin 2\varphi$, anomalous current and direction dependent critical current is shown.

DOI: 10.1038/NPHYS3742

4. Shifts of the SQUID phase shift pattern

In order to understand the origin of the shifts in our SQUID patter, we have performed simulations of the critical current of a dc-SQUID consisting of two Josephson junctions with current-phase relationships (CPR) $I_{S_{1,2}} = \mathrm{CPR}_{1,2}(\varphi_{1,2})$, where $I_{S_1}(I_{S_2})$ is the switching current of junction 1 (junction 2) and $\varphi_1(\varphi_2)$ is the superconducting phase difference across junction 1 (junction 2).

Assuming negligible SQUID inductance, the phase difference across the junctions are related to each other by the equation $\varphi_2 = \varphi_1 - 2\pi\frac{\Phi_{ext}}{\Phi_0}$, where Φ_{ext} is the external flux applied through the SQUID. The critical current of the SQUID is the calculated using the equation

$$I_{C,SQUID} = \max_{\varphi}\left|\mathrm{CPR}_1(\varphi) + \mathrm{CPR}_2\left(\varphi - 2\pi\frac{\Phi_{ext}}{\Phi_0} + 2\pi n\right)\right|.$$

In Fig. S5 **(a)** we plot the critical current of the SQUID assuming $I_{S_{1,2}} = I_{C_{1,2}}\sin\varphi_{1,2}$ for several values of the ratio $\frac{I_{C_1}}{I_{C_2}}$. We observe that although the shape of the $I_{C,SQUID}$ vs flux curve varies, the points in flux of the maxima and minima are fixed. In Fig. S5 **(b)** we plot the same curves but now CPR_1 is a periodic sawtooth, i.e. $I_{S_1} = I_{c_1}\left(\frac{1}{\pi}\varphi - 1\right)$. Still the minima and the maxima of the critical current remain fixed, independent of the ratio $\frac{I_{C_1}}{I_{C_2}}$.

In Fig. S5 (**c**) we assume $I_{S_1} = 0.1I_{C_2}\sin(\varphi_1 - \varphi_0)$ and vary the value of φ_0. In contrast to the previous two cases, the maxima and minima of the critical current now shift by $\Phi_{ext} = \frac{\varphi_0}{2\Pi}$. Considering that the maximum (minimum) of $I_{C,SQUID}$ corresponds to a minimum (maximum) in the measured voltage V over the SQUID, such $I_{C,SQUID}$ behaviour is qualitatively similar to the measured voltage pattern shown in Fig 3. (**b**), (**c**) and Fig. 4 of the main text as well as Fig S6 (**b**) of this supplementary. In our simulations the only way we could induce additional phase shifts in the SQUID pattern is to offset one of the junctions by φ_0. Therefore these are consistent with our interpretation that the origin of the shift in our measured SQUID patterns is indeed a consequence of the shift by φ_0 in CPR of the nanowire Josephson junction.

To be certain that the magnitude of the critical currents does not influence the phase of the SQUID oscillations, we repeated scans with the same gate voltages over the quantum dot V_1, V_2, V_3, and varied $I_{C_{ref}}$ by changing the gate voltage of the reference junction V_{ref} over a wide range and found no change of the induced shift, even when the SQUID is underdamped regime.

This is understandable since the phase difference between the junctions in a SQUID geometry is fixed by the external flux. So while the relative ratio between the critical currents (which is not exactly known due to phase diffusion) have impact on the critical current values and in general on the visibility of the SQUID response they do not change the phase offset. This fact is illustrated in the experiment of *Spathis et al.* [8], where the authors measured the nanowire SQUID response in the wide range of temperatures and found no shifts in the pattern.

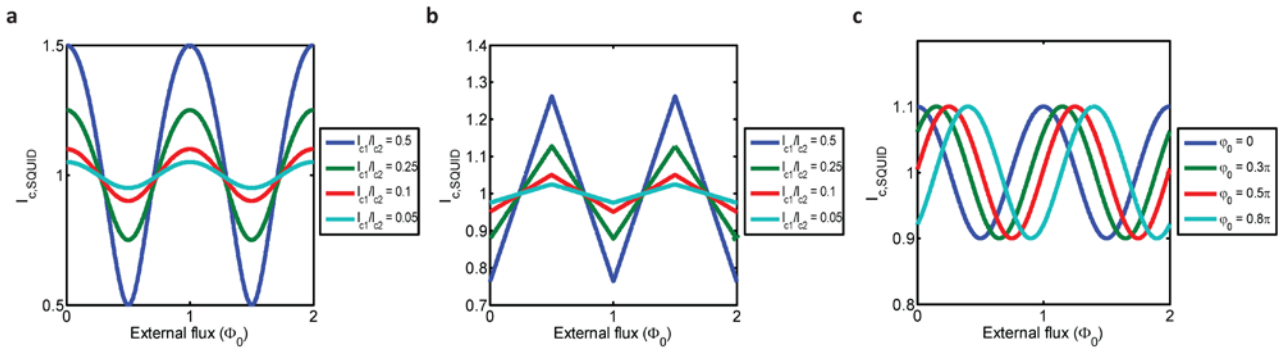

Fig. S5: Critical current simulations of a dc-SQUID | a, Simulation including two sinusoidal junctions with varying critical current ratios. **b**, Simulation including a junction 1 with a sawtooth-like CPR and junction 2 with a sinusoidal CPR, with varying critical current ratios. **c**, Simulation including two sinusoidal junctions where the CPR of junction 1 is shifted by a phase φ_0. The ratio $\frac{I_{C_1}}{I_{C_2}} = 0.1$.

DOI: 10.1038/NPHYS3742

5. Additional data

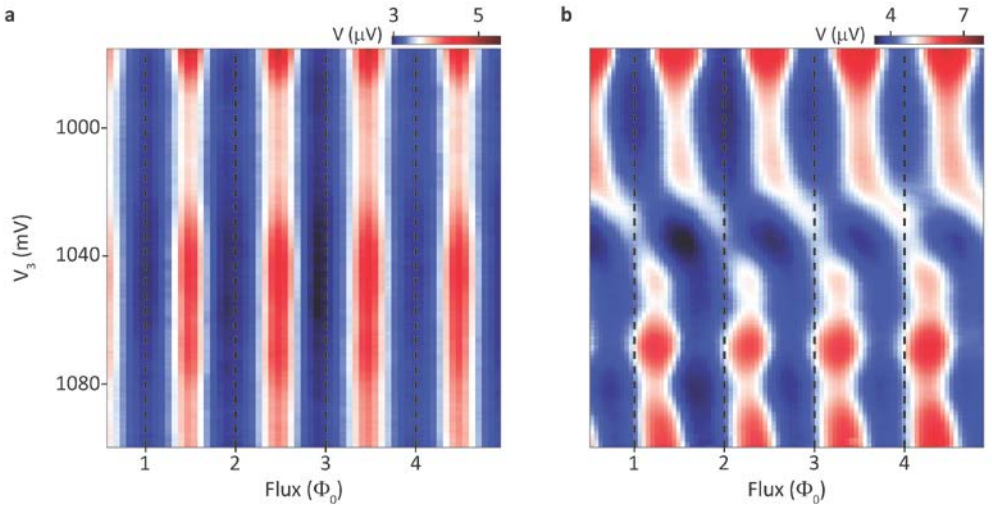

Fig. S6: Measured voltage as a function of flux and V_3 | a, $B_{\text{in-plane}} = 0$. **b**, $B_{\text{in-plane}} = 150$ mT, θ=75°. In this regime no 0-π transition is observed suggesting that multiple quantum dot orbitals contribute to the transport. The phase shifts are mainly constant inside the regions of gate space in which the quantum dot occupation number is fixed. Gate settings are: $V_1 = 100$ mV; $V_2 = 50$ mV; $I_{\text{bias}} = 220$ pA; $V_{\text{ref}} = 450$ mV.

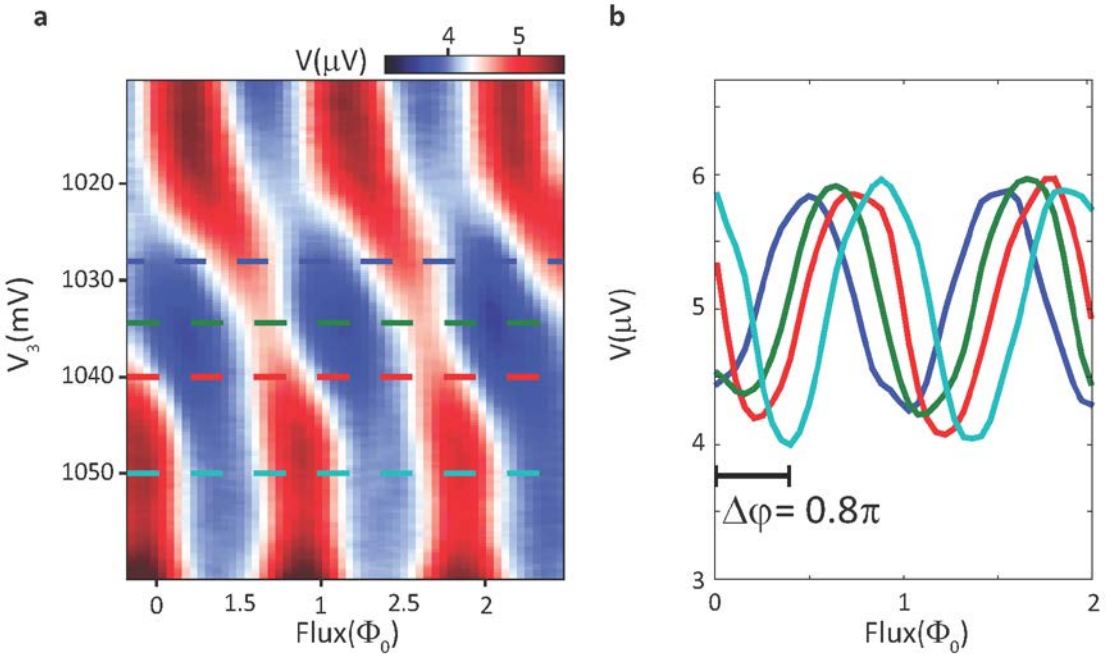

Fig. S7: Continuously gate tunable φ_0-shift | a: zoom in on Fig. S6 (**b**). The dashed lines represent the values of V_3 at which the curves in (**b**) are taken. **b**, Measured voltage vs flux taken at consecutive V_3 values marked in (**a**). The total phase shift between the blue curve and cyan curve is 0.8π.

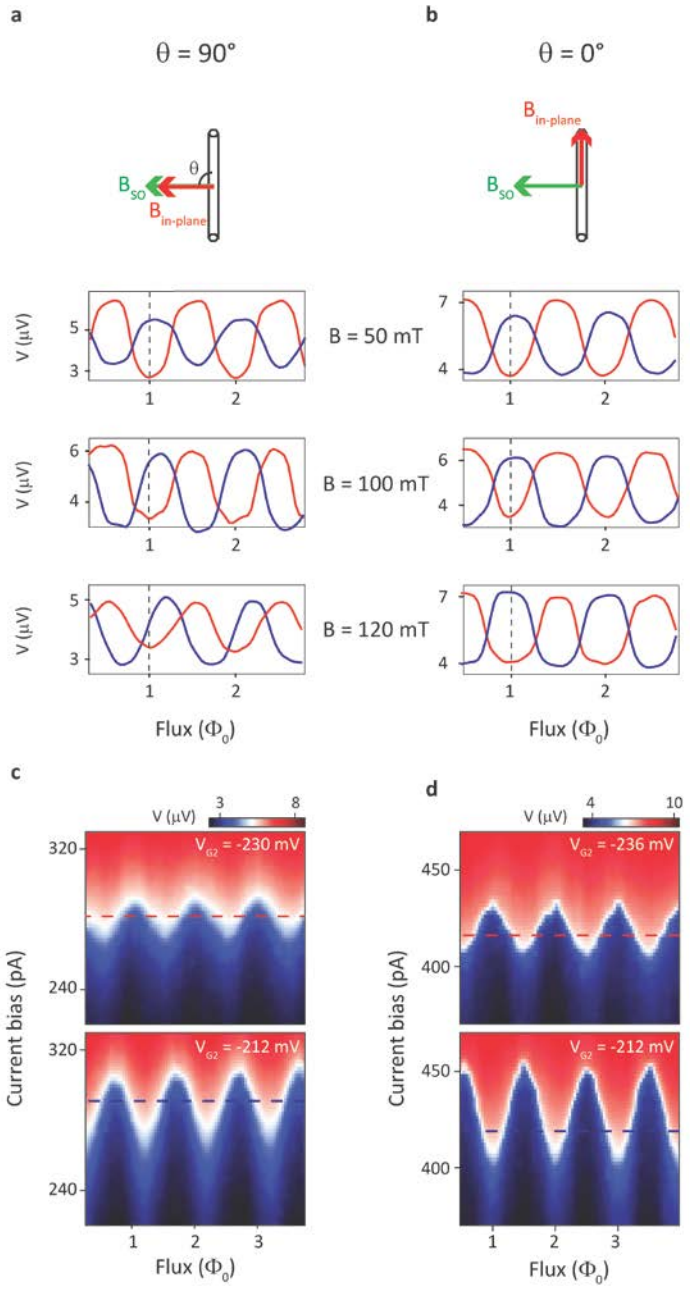

Fig. S8: Evolution of the shift in the SQUID pattern with the magnetic field for two different magnetic field orientations | a, orthogonal to the nanowire. **b,** Along the nanowire. The blue and red traces correspond to the two consecutive quantum dot occupation states. **c**,**d**, Voltage as a function of flux and current bias at $B_{\text{in-plane}}$ = 120 mT for the same field orientation as in (**a**) and (**b**). The sharp transition from the low voltage state (blue) to the high voltage state (red) indicates the value of the switching current as a function of flux. The phase offset is independent of the current bias. The red and blue lines correspond to the current bias at which the data in the lowest panel of (**a**) and (**b**) is taken.

DOI: 10.1038/NPHYS3742

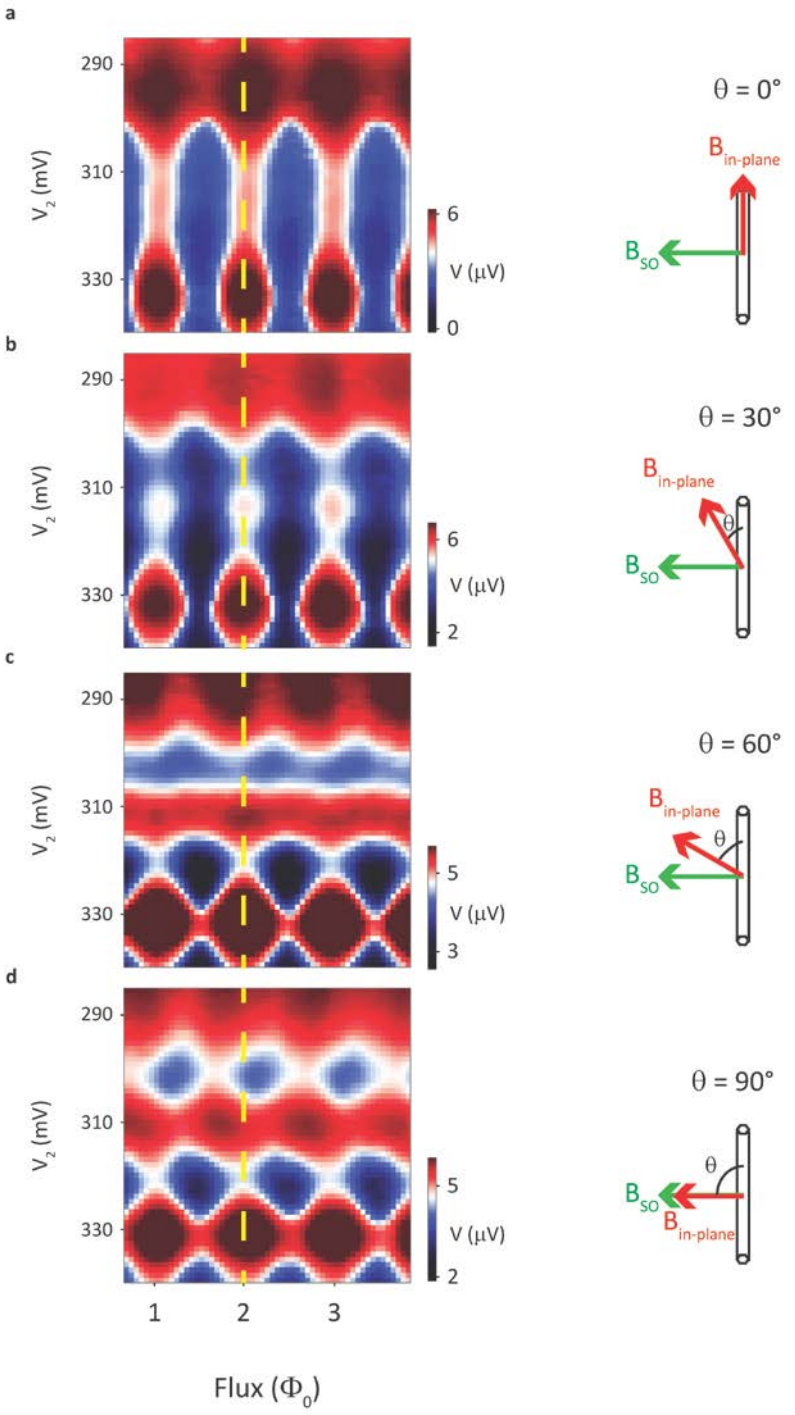

Fig. S9: Anisotropy of the SQUID phase shift in the open QD regime | a-d, Voltage as a function of V_2 and flux for different orientations of $\boldsymbol{B}_{\text{in-plane}}$ and **30-50** more electrons compared to the regime in Fig. 4. Here the 0-π transition was not observed strongly suggesting that multiple orbitals are contributing to the transport. In this very different regime compared to the data discussed in the main text the φ_0 shifts are still the largest when the external in-plane field ($B_{\text{in-plane}}$= 100mT) is oriented orthogonal to the nanowire.

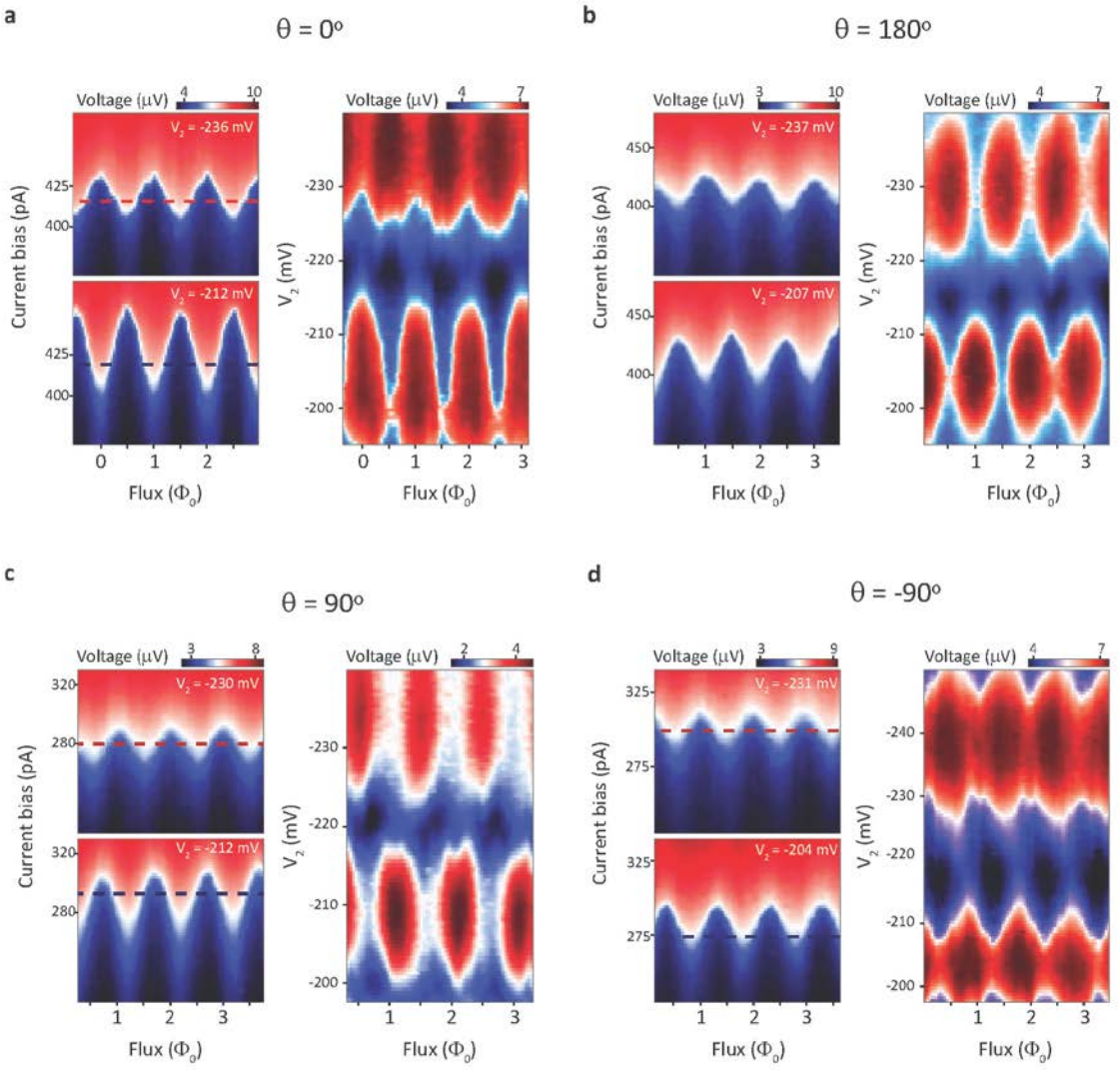

Fig. S10: Additional anisotropy data for $B_{\text{in-plane}}$ = 120 mT | a-d, The left panel shows voltage vs current bias and flux for the gate settings corresponding to two consecutive Coulomb blockade regions. The right panel shows voltage vs V_2 and flux. The angle θ between the nanowire and $\mathbf{B}_{\text{in-plane}}$ is indicated. Blue and red dashed lines indicate cuts shown in Fig. 4. The corresponding values of the I_{bias} are: (**a**) top panel I_{bias} = 415 pA , bottom panel I_{bias} = 420 pA; (**c**) I_{bias} = 280 pA, I_{bias} = 290 pA; (**d**) I_{bias} = 295 pA, I_{bias} = 275 pA.

DOI: 10.1038/NPHYS3742

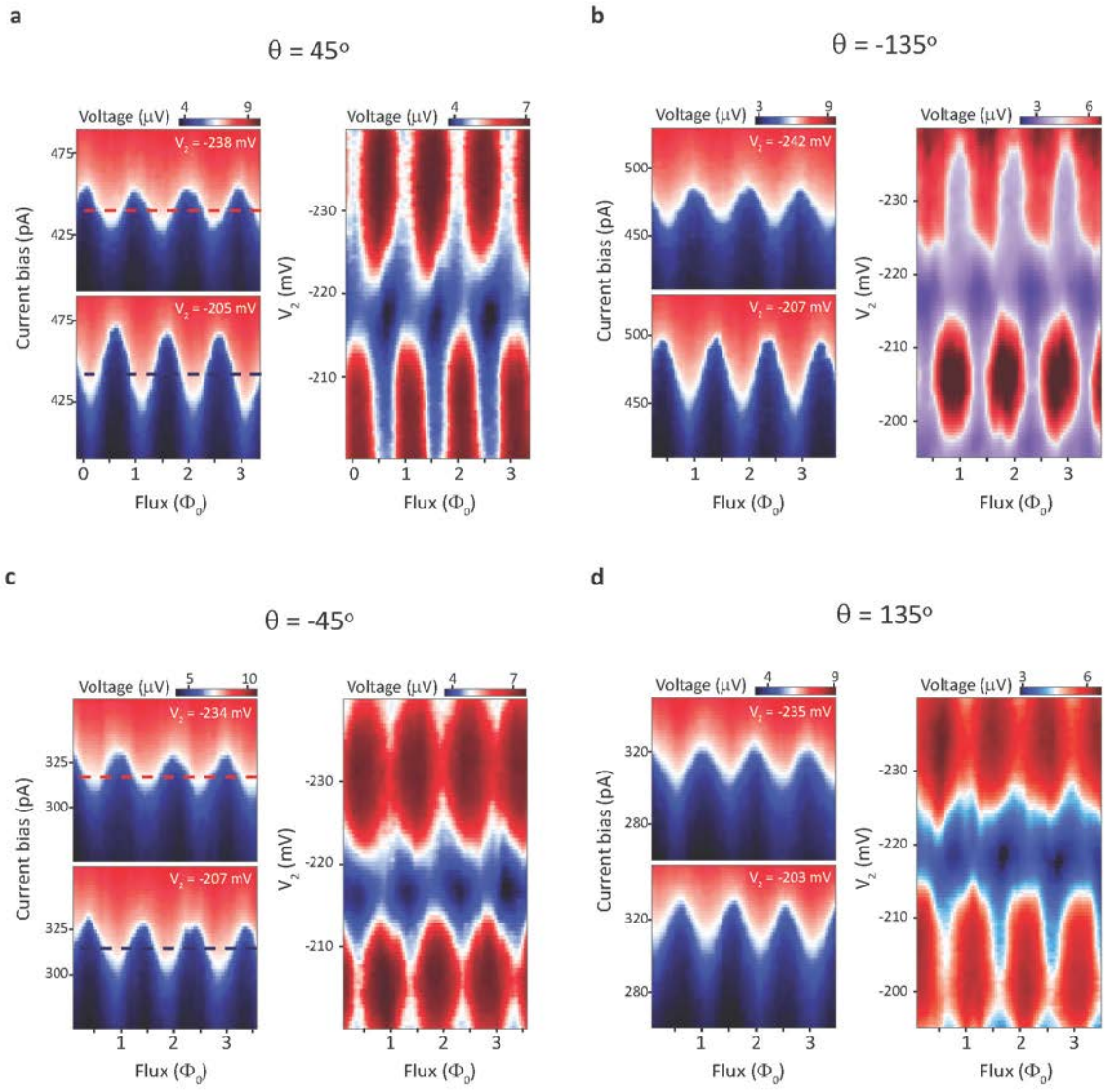

Fig. S11: Additional anisotropy data for $B_{\text{in-plane}}$ = 120 mT | a-d,The Left panel shows voltage vs current bias and flux for the gate settings corresponding to two consecutive Coulomb blockade regions. The right panel shows voltage vs V_2 and flux. The angle θ between the nanowire and $\mathbf{B}_{\text{in-plane}}$ is indicated. Blue and red dashed lines indicate cuts shown in Fig. 4. The corresponding values of the I_{bias} are: (**a**) top panel I_{bias} = 440 pA , bottom panel I_{bias} = 440 pA; (**c**) I_{bias} = 320 pA, I_{bias} = 315 pA.

6. Establishing the origin of the shift in the SQUID pattern

Our main experimental observations can be summarized as follows: (1) the observed shift in the SQUID pattern occurs for a finite in-plane magnetic field which exact value depends on the QD configuration; (2) the shift in pattern occurs mainly for gate values at which the QD electron occupation number changes; (3) the shift is the largest when the field is orthogonal to the nanowire and almost non-existing when the field is oriented along the nanowire.

These observations are qualitatively in agreement with SOI induced orbital mixing as the origin of the φ_0–junction. Based on (1) and (2) it is evident that QD orbital levels play a crucial role in the superconducting transport which is also in agreement with previous experiments on quantum dots [9–11]. Also, the observed anisotropy is consistent with reported SOI direction in QDs [12]. In the following we discuss other effects which may also contribute to the observed shifts in the SQUID pattern.

a) Gate induced changes in the effective SQUID area. Gating off a part of the wire changes the effective SQUID area which may result in additional shifts of the interference pattern. This effect is rather small in our devices. The maximal change in the area, and therefore the phase offset, would be at most few percent estimated by comparing the gated nanowire area 100nm x 100nm with the total area of the SQUID. Even if assumed that the magnetic field is enhanced in the vicinity of the nanowire junction, due to complicated field profile caused by the nearby superconductor, the change in area has to be extremely large to account for the observed shift. Also, for substantial changes in the area, the flux periodicity of the SQUID response has to change substantially. These changes were not observed in the experiment which shows periodicity of 1.2mT being independent of the gate parameters. We also note that we didn't observe any discontinuous jumps in the interference pattern while sweeping the magnetic field which rules out phase shifts due to accidental events of flux trapping in the junction.

b) Phase offsets due to flux in the quantum dot. The observed shifts in the SQUID pattern were obtained in in-plane field values of 50-100 mT. Assuming the quantum dot area to be 60nm x 60nm (corresponding to E_{orb} = 1.5 meV), the total flux through the corresponding area would be of the order of 0.1-0.2 Φ_0. Based on this estimate, even if the flux through the QD would fully add to the φ_0 offset, the resulting shift would be too small to explain the experimental data. Note that we verified that there is no significant modification of the field profile in the vicinity of the quantum dot by measuring the values of the g-factors.

c) Additional orbital effects. As discussed in Ref. [5,6], when the tunnelling coefficients (matrix elements) describing the hybridization between the QD levels and the left (right) lead are complex numbers and contribute to additional phase factors, at finite magnetic field an anomalous Josephson current may occur. Orbital effects can also contribute to this complex phase instead of SOI. While this is in principle a possible scenario it is not consistent with the experimental data as one would not expect any magnetic field anisotropy in this case. Another possible scenario is that orbital effects alone can result in an anomalous current. As pointed out in Refs. [13,14] orbital effects alone may have a significant influence on superconducting transport through the nanowire without any QD. Although these effects may indeed contribute, they are to the large degree linear in magnetic field strength in contrast to the experimental data. For this reason, we can rule out these effects as the main contribution of the observed shifts.

DOI: 10.1038/NPHYS3742

7. Estimation of the anomalous current

Using the data from the regime presented in Fig. S8 (**a**) and the relation $I_{anomalous} = I_C \sin\varphi_0$**,** we estimate the minimum anomalous current through our quantum dot.

The procedure we use the estimate the anomalous current goes as following. We assume that the critical current I_C is constant along charge state transitions for a fixed $\boldsymbol{B}_{\text{in-plane}}$. Within a charge transition where we measure a relative change in phase of φ_0, we choose the larger value of the possible magnitude of the anomalous current, i.e. $\max(|I_C \sin\varphi|, |I_C \sin(\varphi + \varphi_0)|)$. However, since the phase difference φ across the quantum dot is unknown, we minimize this function over all possible values of φ. Thus we obtain our minimum estimate of the magnitude of the anomalous current $|I_{\min\_anomalous}|$ as

$$|I_{\min\_anomalous}| = \min_{\varphi\in[0,\pi]}\{\max(|I_C \sin\varphi|, |I_C \sin(\varphi + \varphi_0)|)\}.$$

$|I_{\min\_anomalous}|$ vanishes for $\varphi_0 = 0, \pi$ as expected for zero and π-junctions, and is positive otherwise. Fig. S12 shows the values extracted for particular φ_0-shifts measured. Note that shift is non-linear function of the field. While for a small magnitude values of $\boldsymbol{B}_{\text{in-plane}}$ the anomalous current is negligible, above certain critical value of the field the shift abruptly increases.

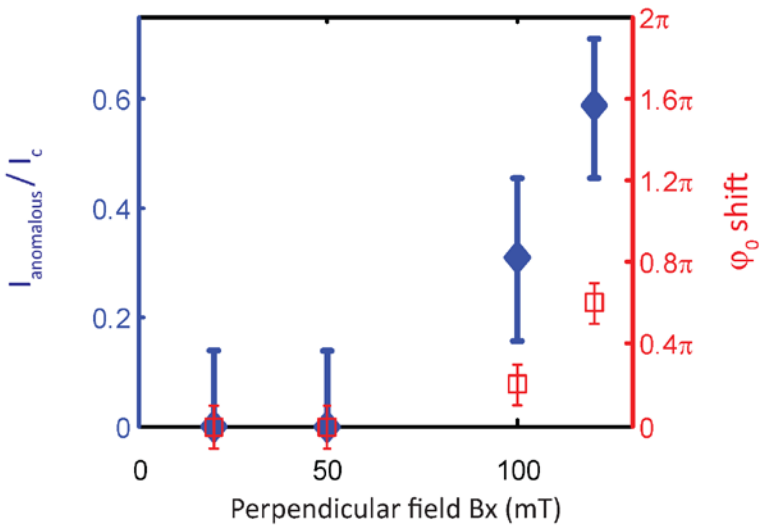

Fig. S12: Anomalous current as a function of magnetic field | Estimates and measured phase shifts of $I_{\text{anomalous}}$ as a function of field magnitude for the regime shown in S8 (perpendicular in-plane field).

References:

1. Reynoso, A. A., Usaj, G., Balseiro, C. A., Feinberg, D. & Avignon, M. Anomalous Josephson Current in Junctions with Spin Polarizing Quantum Point Contacts. *Phys. Rev. Lett.* **101,** 107001 (2008).

2. Yokoyama, T., Eto, M. & Nazarov, Y. V. Anomalous Josephson effect induced by spin-orbit interaction and Zeeman effect in semiconductor nanowires. *Phys. Rev. B* **89,** 195407 (2014).

3. Dolcini, F., Houzet, M. & Meyer, J. S. Topological Josephson φ_0 junctions. *Phys. Rev. B* **92,** 035428 (2015).

4. Dell'Anna, L., Zazunov, A., Egger, R. & Martin, T. Josephson current through a quantum dot with spin-orbit coupling. *Phys. Rev. B* **75,** 085305 (2007).

5. Zazunov, A., Egger, R., Jonckheere, T. & Martin, T. Anomalous Josephson Current through a Spin-Orbit Coupled Quantum Dot. *Phys. Rev. Lett.* **103,** 147004 (2009).

6. Brunetti, A., Zazunov, A., Kundu, A. & Egger, R. Anomalous Josephson current, incipient time-reversal symmetry breaking, and Majorana bound states in interacting multilevel dots. *Phys. Rev. B* **88,** 144515 (2013).

7. Feynman, R. P., Leighton, R. B. & Sands, M. *THE FEYNMAN LECTURES ON PHYSICS, Vol III, Quantum Mechanics*. (Addison-Wesley Publishing Company, Inc., 1965).

8. Spathis, P. *et al.* Hybrid InAs nanowire–vanadium proximity SQUID. *Nanotechnology* **22,** 105201 (2011).

9. van Dam, J. A., Nazarov, Y. V., Bakkers, E. P. A. M., De Franceschi, S. & Kouwenhoven, L. P. Supercurrent reversal in quantum dots. *Nature* **442,** 667–670 (2006).

10. Jarillo-Herrero, P., van Dam, J. A. & Kouwenhoven, L. P. Quantum supercurrent transistors in carbon nanotubes. *Nature* **439,** 953–956 (2006).

11. De Franceschi, S., Kouwenhoven, L., Schönenberger, C. & Wernsdorfer, W. Hybrid superconductor-quantum dot devices. *Nat. Nanotechnol.* **5,** 703–711 (2010).

12. Nadj-Perge, S. *et al.* Spectroscopy of Spin-Orbit Quantum Bits in Indium Antimonide Nanowires. *Phys. Rev. Lett.* **108,** 166801 (2012).

13. Gharavi, K. *et al.* Josephson Interference due to Orbital States in a Nanowire Proximity Effect Junction. *ArXiv14057455 Cond-Mat* (2014). at <http://arxiv.org/abs/1405.7455>

14. Gharavi, K. & Baugh, J. Orbital Josephson interference in a nanowire proximity-effect junction. *Phys. Rev. B* **91,** 245436 (2015).

15. Sickinger, H. *et al.* Experimental Evidence of a φ Josephson Junction. *Phys. Rev. Lett.* **109,** 107002 (2012).

16. Brunetti, A., Zazunov, A., Kundu, A. & Egger, R. Anomalous Josephson current, incipient time-reversal symmetry breaking, and Majorana bound states in interacting multilevel dots. *Phys. Rev. B* **88,** 144515 (2013).

17. Yokoyama, T., Eto, M. & V. Nazarov, Y. Josephson Current through Semiconductor Nanowire with Spin–Orbit Interaction in Magnetic Field. *J. Phys. Soc. Jpn.* **82,** 054703 (2013).

18. Mal'shukov, A. G., Sadjina, S. & Brataas, A. Inverse spin Hall effect in superconductor/normal-metal/superconductor Josephson junctions. *Phys. Rev. B* **81,** 060502 (2010).

19. Krive, I. V., Kadigrobov, A. M., Shekhter, R. I. & Jonson, M. Influence of the Rashba effect on the Josephson current through a superconductor/Luttinger liquid/superconductor tunnel junction. *Phys. Rev. B* **71,** 214516 (2005).

20. Braude, V. & Nazarov, Y. V. Fully Developed Triplet Proximity Effect. *Phys. Rev. Lett.* **98,** 077003 (2007).

21. Tanaka, Y., Golubov, A. A., Kashiwaya, S. & Ueda, M. Anomalous Josephson Effect between Even- and Odd-Frequency Superconductors. *Phys. Rev. Lett.* **99,** 037005 (2007).

22. Eschrig, M. *et al.* Symmetries of Pairing Correlations in Superconductor–Ferromagnet Nanostructures. *J. Low Temp. Phys.* **147,** 457–476 (2007).

23. Tanaka, Y., Yokoyama, T. & Nagaosa, N. Manipulation of the Majorana Fermion, Andreev Reflection, and Josephson Current on Topological Insulators. *Phys. Rev. Lett.* **103,** 107002 (2009).

24. Dolcini, F., Houzet, M. & Meyer, J. S. Topological Josephson φ_0 junctions. *Phys. Rev. B* **92,** 035428 (2015).

25. Yip, S. Josephson current-phase relationships with unconventional superconductors. *Phys. Rev. B* **52,** 3087–3090 (1995).

26. Tanaka, Y. & Kashiwaya, S. Theory of Josephson effects in anisotropic superconductors. *Phys. Rev. B* **56,** 892–912 (1997).

27. Sigrist, M. Time-Reversal Symmetry Breaking States in High-Temperature Superconductors. *Prog. Theor. Phys.* **99,** 899–929 (1998).